Molecular Neurobiology (2019) 56:6873–6882
https://doi.org/10.1007/s12035-019-1579-1

Impaired Remyelination in a Mouse Model of Huntington Disease

Roy Tang Yi Teo[1] · Costanza Ferrari Bardile[1] · Yi Lin Tay[1] · Nur Amirah Binte Mohammad Yusof[1] · Charbel A. Kreidy[1] · Liang Juin Tan[1] · Mahmoud A. Pouladi[1,2,3]

Received: 6 February 2019 / Accepted: 20 March 2019 / Published online: 2 April 2019

Abstract

White matter (WM) abnormalities are a well-established feature of Huntington disease (HD), although their nature is not fully understood. Here, we asked whether remyelination as a measure of WM plasticity is impaired in a model of HD. Using the cuprizone assay, we examined demyelination and remyelination responses in YAC128 HD mice. Treatment with 0.2% cuprizone (CPZ) for 6 weeks resulted in significant reduction in mature (GSTπ-positive) oligodendrocyte counts and FluoroMyelin staining in the corpus callosum, leading to similar demyelination states in YAC128 and wild-type (WT) mice. Six weeks following cessation of CPZ, we observed robust remyelination in WT mice as indicated by an increase in mature oligodendrocyte counts and FluoroMyelin staining. In contrast, YAC128 mice exhibited an impaired remyelination response. The increase in mature oligodendrocyte counts in YAC128 HD mice following CPZ cessation was lower than that of WT. Furthermore, there was no increase in FluoroMyelin staining compared to the demyelinated state in YAC128 mice. We confirmed these findings using electron microscopy where the CPZ-induced reduction in myelinated axons was reversed following CPZ cessation in WT but not YAC128 mice. Our findings demonstrate that remyelination is impaired in YAC128 mice and suggest that WM plasticity may be compromised in HD.

Keywords Huntington disease · White matter · Myelination · Oligodendrocytes · Plasticity

Introduction

Myelin sheaths are among the most specialized forms of plasma membrane found in vertebrates [1]. Along with the oligodendrocytes that produce them, they play a critical role in central nervous system (CNS) function by facilitating efficient neurotransmission and supporting energetic demands of axons [1]. While the majority of oligodendrocytes are generated early in post-natal development [2], a substantial population of proliferative and largely self-sustaining oligodendroglia progenitors remains undifferentiated in the mature CNS [3]. In the healthy adult brain, oligodendrocytes are formed continuously from this pool of cells, fueling important processes such as myelin remodeling, internode replacement, adaptive myelination during skill acquisition, and remyelination during aging [4]. Indeed, while most myelination occurs early in life as part of an innate program of myelin development [5], myelination processes are still very relevant in the adult brain, allowing it to exhibit considerable plasticity and, more crucially, to combat a range of metabolic and immune insults which can cause demyelination and lead to neurodegeneration [6, 7]. Thus, impairments in white matter (WM) plasticity in adulthood would be expected to contribute to neurological dysfunction.

Huntington disease (HD) is a progressive neurodegenerative disorder and the most common genetic cause of dementia [8]. The disease is characterized by a constellation of motor, cognitive, and psychiatric features and remains without a cure. Research efforts to date have largely focused on dissecting the pathogenic processes leading to the prominent atrophy of the caudate and putamen seen in the disease [9, 10]. Recent evidence however also points to WM pathology as an early and potentially primary deficit in HD. Longitudinal imaging studies have shown progressive WM atrophy in prodromal individuals carrying the HD mutation as well as patients in early

Electronic supplementary material The online version of this article (https://doi.org/10.1007/s12035-019-1579-1) contains supplementary material, which is available to authorized users.

✉ Mahmoud A. Pouladi
map@pouladilab.org

[1] Translational Laboratory in Genetic Medicine, Agency for Science, Technology and Research, Singapore (A*STAR), 8A Biomedical Grove, Immunos, Level 5, Singapore 138648, Singapore

[2] Department of Medicine, National University of Singapore, Singapore 117597, Singapore

[3] Department of Physiology, National University of Singapore, Singapore 117597, Singapore

stages of disease [11–15]. Imaging studies have further shown that WM abnormalities correlate with the length of the etiologic *HTT* CAG repeat expansion in patients with HD [16]. We and others have also shown that WM and myelination abnormalities appear early during development and before the manifestation of behavioral deficits and neuronal atrophy in murine models of HD [17–22]. However, it is not clear whether WM plasticity is affected in HD.

Here, we examined the remyelination response following a demyelinating insult in the YAC128 mouse model of HD [23] as a measure of WM plasticity. The YAC128 mice express the full-length human *HTT* gene and recapitulate key features of the disease, including early WM abnormalities [20, 24]. We employed cuprizone (CPZ) treatment, a well-characterized model of demyelination [25], to cause degeneration of mature myelinating oligodendrocytes and demyelination in wild-type (WT) and YAC128 HD mice. Cessation of CPZ treatment allows regeneration of oligodendrocytes from oligodendrocyte progenitor cells and for remyelination to take place [25]. By evaluating the density of mature oligodendrocytes, the myelinated area, and the proportion of myelinated axons in the corpus callosum, the largest WM structure in the brain, we were able to compare the demyelination state and remyelination response between WT and YAC128 HD mice. Our findings indicate a compromised remyelination response in YAC128 mice and suggest that WM plasticity may be impaired in HD.

Material and Methods

Animals Male YAC128 HD mice (line 53) expressing a full-length human HTT transgene with 128 CAG repeats maintained on the FVB/N strain were used [23]. Mice were housed with littermates of mixed genotype in groups of 2–5 on a 12-h light/dark cycle with free access to food and water. All experiments were performed with the approval of the Institutional Animal Care and Use Committee (IACUC no. 151067) at Biological Resource Centre (BRC), A*STAR.

Cuprizone Treatment Cuprizone (Sigma) (0.2%) was pelleted in Teklad 2918 feed (Harlan). Eight- to ten-week old mice were allowed to feed ad libitum, and the pellets were changed every 2 days for 6 weeks. For recovery, the mice were switched to the normal pelleted Teklad 2918 (Harlan) diet for a further 6 weeks.

Immunohistochemistry and Stereological Measurements The mouse brains were removed and left in 4% paraformaldehyde overnight before being washed three times with PBS. They were then transferred to a 30% sucrose solution containing 0.08% sodium azide in PBS for cryoprotection. After the brains had sunk (~24 h), they were weighed, snap frozen in isopentane chilled with dry ice, and stored at − 80 °C. The brains were mounted with Tissue-TEK O.C.T. compound (Sakura, Torrance, CA, USA) and sliced coronally into 25-μm sections on a cryostat (Microm HM 525, Thermo Scientific) and were collected from approximately Bregma 1.10 to − 0.22 free floating in PBS with 0.08% sodium azide before storage at 4 °C. A series of 9-12 coronal sections spaced 600 μm apart were stained with a primary rabbit antibody against GSTπ (MBL no. 311) overnight at 4 °C, followed by incubation with a biotinylated anti-rabbit antibody (1:200; Vector Laboratories, Burlingame, CA, USA). The signal was amplified with an ABC Elite kit (Vector) and detected with diaminobenzidine (Pierce). Cell counts in the corpus callosum were determined from a series of mounted sections using StereoInvestigator software (Microbrightfield, Williston, VT, USA) by tracing the perimeter of the corpus callosum in serial sections. To visualize myelin, FluoroMyelin (Thermofisher) was used with the manufacturer's protocol adapted for our usage. Briefly, the slices were permeabilized in PBS with 0.2% Triton X-100 for 40 min before incubating in FluoroMyelin (1:400) for 30 min. After washing in PBS, the slices were mounted on slides and visualized with a Nikon Ni-E upright microscope.

Transmission Electron Microscopy Mice were transcardially perfused with 2.5% glutaraldehyde and 2.5% PFA in 0.1 M sodium cacodylate buffer before post-fixing the brains overnight at 4 °C in the same buffer, and then subsequently washing in phosphate-buffered saline. Brain samples were sent to the Harvard Medical School EM unit for further processing. Briefly, coronal slices at the level of Bregma − 1 mm were made from the central part of the corpus callosum before post fixation in a 1% osmium tetroxide and 1.5% potassium ferrocyanide solution for 1 h. After washing with a 1% uranyl acetate in maleate buffer, the samples were dehydrated, infiltrated with epon, embedded and polymerized at 60 °C for 2 days. Ultra-thin slices (100 nm) were cut before imaging on a TEM. For image analyses, StereoInvestigator v11 was employed to allow for systematic random selection of axons, with ~ 150 axons analyzed per brain.

Statistics

Data are expressed as means ± SEM. Statistical significance was determined by one- or two-way ANOVA with Fisher's LSD post hoc test. Cumulative frequencies of g-ratios were analyzed using the unpaired two-tailed Kolmogorov-Smirnov test. Differences were considered statistically significant when $p < 0.05$.

Results

CPZ treatment is a well-characterized and widely used experimental approach to study oligodendrogenesis and myelination in adulthood [25]. In this assay, acute CPZ treatment causes degeneration of mature oligodendrocytes and subsequent demyelination. These effects of CPZ are thought to be induced by copper chelation which results in enzymatic and metabolic dysfunction leading to elevated oxidative and ER stress along with amino acid deficits and disturbed myelin lipid and protein synthesis [25]. These abnormalities, which appear to affect mature oligodendrocytes preferentially, ultimately result in disintegration of myelin sheath and induction of apoptosis [25]. Following cessation of CPZ, oligodendrogenesis is stimulated in the adult brain and results in recovery through de novo myelination [25]. We treated YAC128 and WT littermates with a CPZ-supplemented diet and assayed their myelination status after 6 weeks of treatment (Fig. 1). The density of GSTπ+ mature oligodendrocytes was significantly lower in control YAC128 HD compared with WT mice (Fig. 2a, Supplementary Fig. 1A–C). Treatment with CPZ resulted in a significant decrease in GSTπ+ mature oligodendrocyte densities in both WT and YAC128 mice compared to their respective controls (Fig. 2a). Furthermore, the densities of GSTπ+ oligodendrocytes were not different between YAC128 and WT mice following CPZ treatment (Fig. 2a).

We next evaluated the extent of demyelination in the corpus callosum by staining with FluoroMyelin, a fluorescent dye that has selectivity for myelin (Fig. 2b) [26]. CPZ treatment resulted in demyelination as indicated by the significant decrease in the area of FluoroMyelin-positive staining in both WT and YAC128 mice compared to their respective controls (Fig. 2c). The extent of demyelination, which largely reflects loss of myelin in the external capsule region of the corpus callosum, was similar between WT and YAC128 HD mice (Fig. 2c). There was no difference in area of FluoroMyelin-positive staining between YAC128 and WT mice at baseline, consistent with the lack of corpus callosum atrophy in YAC128 HD mice at this age range [17]. We also assessed the intensity of FluoroMyelin staining which reflects myelin content. While CPZ treatment resulted in a marked decrease in WT mice compared to corresponding controls, no difference was seen between CPZ- and control-treated YAC128 HD mice (Fig. 2d). There was no difference in the intensity of FluoroMyelin staining between WT and YAC128 following CPZ treatment (Fig. 2d). These results indicate that CPZ treatment leads to similar demyelinated states in YAC128 HD and WT mice.

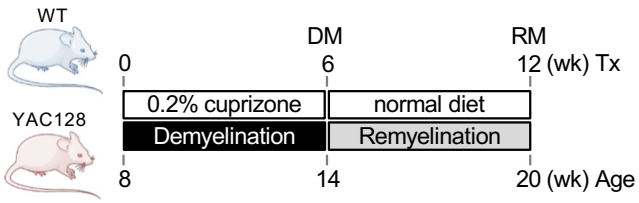

Fig. 1 Experimental design of the cuprizone demyelination assay. To induce demyelination, 8-week-old YAC128 HD and littermate WT mice were placed on a 0.2% cuprizone diet for 6 weeks (wk). To allow for spontaneous remyelination, cuprizone diet was replaced with control diet for 6 additional weeks. DM = demyelinated, RM = remyelinated, Tx = treatment

Following demyelination, cessation of CPZ treatment leads to recovery and remyelination [25]. On the cellular level, the densities of GSTπ+ mature oligodendrocytes increased significantly following CPZ cessation in both WT and YAC128 HD mice (Fig. 3a). However, the increase in WT mice was significantly greater than in YAC128 HD mice (Fig. 3a). Staining with FluoroMyelin (Fig. 3b) showed that while the myelin-positive area was significantly increased following CPZ cessation in both WT and YAC128 HD mice (Fig. 3c), the amount of myelin as represented by the intensity of the FluoroMyelin-positive staining increased in WT mice only (Fig. 3d). These results indicate that remyelination is compromised in YAC128 HD mice.

To examine the demyelination and remyelination responses on the ultrastructural level, we performed electron microscopy imaging of the corpus callosum (Fig. 4a–c). Consistent with the changes in GSTπ-positive oligodendrocytes and FluoroMyelin-positive area indicating demyelination, we observed a significant decrease in the percentages of myelinated axons both WT and YAC128 mice post-CPZ treatment (Fig. 4d). Following CPZ cessation and recovery, the percentage of myelinated axons increased significantly in WT mice (Fig. 4d). In contrast, no increase in the percentage of myelinated axons was observed in YAC128 HD following CPZ cessation (Fig. 4d).

Another indicator of remyelination is the presence of thinner myelin sheaths [27]. We evaluated g-ratios, calculated as the ratio of axon caliber to total fiber caliber, as a measure of myelin thickness. In WT mice, cumulative frequency analysis revealed a shift towards higher g-ratio values following cessation of CPZ treatment and recovery, consistent with thinner myelin sheaths and a successful remyelination response (Fig. 4e). A similar phenotype was observed in YAC128 HD mice, with the cumulative frequency curves showing a shift towards higher g-ratio values in the remyelination group compared with the demyelination one (Fig. 4f) indicating thinner myelin sheaths and remyelination. These results suggest that remyelination post-CPZ cessation is present in the YAC128 HD mice, although to a lower extent than that seen in WT mice as indicated by the reduced proportion of myelinated axons observed.

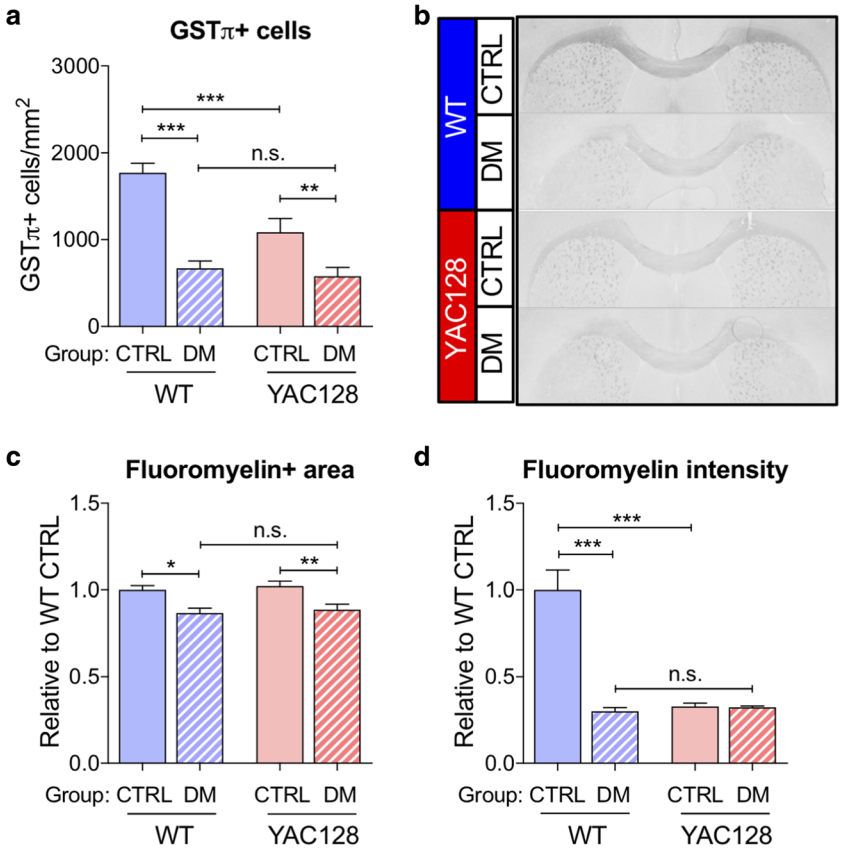

Fig. 2 Cuprizone treatment leads to demyelination in WT and YAC128 HD mice. **a** The density of GSTπ-positive mature oligodendrocytes in the corpus callosum (CC) was significantly lower following cuprizone-induced demyelination (DM) compared to age-matched controls (CTRL) for both WT and YAC128 mice (two-way ANOVA: interaction $p = 0.0163$, genotype $p = 0.0026$, treatment $p < 0.0001$). **b** FluoroMyelin staining of the corpus callosum in control and demyelinated WT and YAC128 mice. Inverted fluorescent images shown. **c** Quantification of FluoroMyelin-positive CC area showing significant demyelination in YAC128 and WT mice (two-way ANOVA: interaction $p = 0.9810$, genotype $p = 0.5166$, treatment $p = 0.0005$). **d** Quantification of the intensity of FluoroMyelin staining in the CC demonstrates significant decrease following demyelination in WT but not YAC128 mice (two-way ANOVA: interaction $p < 0.0001$, genotype $p < 0.0001$, treatment $p < 0.0001$). $N = 4$–7 for WT-CTRL, 4–7 for WT-DM, 5–6 for YAC128-CTRL, and 4–7 for YAC128-DM; Two-way ANOVA with Fisher's LSD post-hoc test. $^{*}p < 0.05$, $^{**}p < 0.01$, $^{***}p < 0.001$, n.s. = not significant

CPZ-induced demyelination is accompanied by an infiltration of microglia and astrocytes which can influence demyelination as well as recovery and remyelination following CPZ cessation [28, 29]. Assessment of Iba1+ cells showed a significantly higher infiltration of microglia following demyelination but similar levels following remyelination in WT compared with YAC128 HD mice (Fig. 5a, Supplementary Fig. 1D–F). In contrast, quantification of GFAP+ cells revealed a similar level of astrogliosis following demyelination but a significantly higher level following remyelination in WT compared with YAC128 HD mice (Fig. 5b, Supplementary Fig. 1G–I). These results suggest that the increase and resolution of Iba1+ microglia are likely to have a minor contribution to the differences in post CPZ-induced recovery between the WT and YAC128 groups. On the other hand, the significantly larger numbers of GFAP+ astrocytes in WT compared to YAC128 mice during the recovery phase indicates that remyelination-promoting astrocytes may contribute to the difference in remyelination observed between WT and YAC128 HD mice.

Discussion

Accumulating evidence points to myelination and WM abnormalities as early pathological features in HD. Imaging studies have demonstrated the presence of WM atrophy and abnormal myelin microstructure in prodromal HD [11, 30–34]. These observations have been recapitulated in animal models of HD where myelin pathology appears during development and precedes neuronal atrophy, implicating primary oligodendroglial dysfunction in these deficits [17–20]. Here, we first show that CPZ treatment leads to similar demyelination states in YAC128 HD and WT mice as measured by mature (GSTπ-positive) oligodendrocyte counts, FluoroMyelin staining, and the proportion of myelinated axons in the corpus callosum. We then demonstrate using these measures that the remyelination response is impaired in YAC128 HD mice. Our findings provide evidence that in addition to the deficits in innate myelination, the ability to remyelinate may be compromised in HD. Our results here are also consistent with our

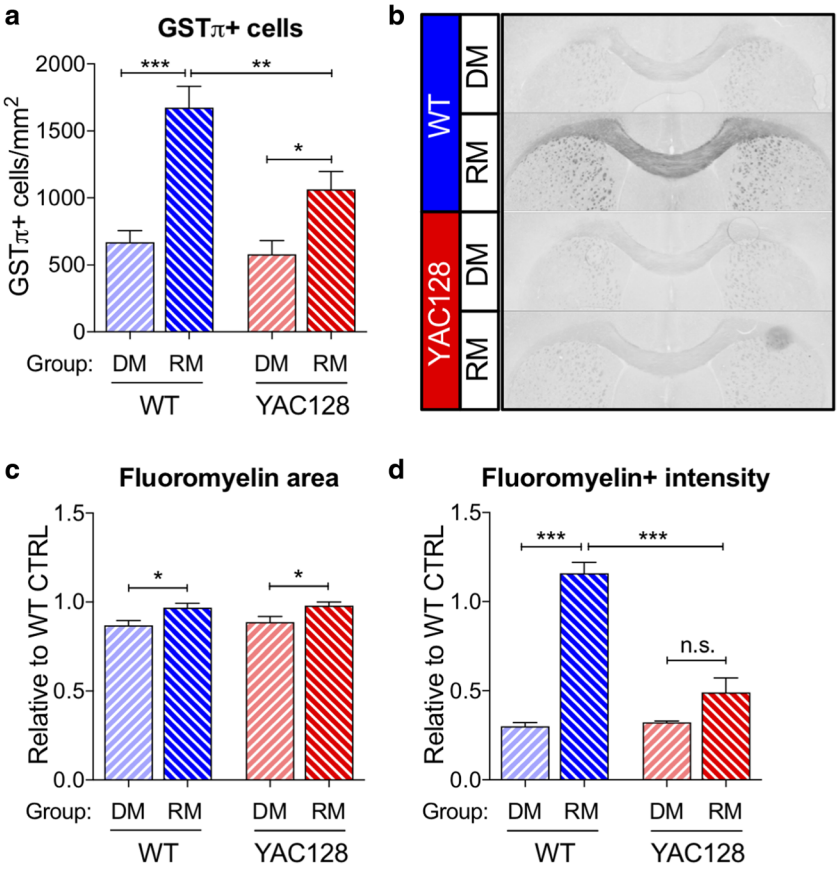

Fig. 3 Remyelination response in the corpus callosum of WT and YAC128 HD mice. **a** The increase in GSTπ-positive mature oligodendrocytes following remyelination was significantly lower in YAC128 HD compared with WT mice (two-way ANOVA: interaction $p = 0.0511$, genotype $p = 0.0108$, treatment $p < 0.0001$). **b** FluoroMyelin staining in demyelinated and remyelinated WT and YAC128 mice. Inverted fluorescent images shown. WT- and YAC128-DM images from Fig. 2 reproduced here for ease of comparison. **c** Quantification of FluoroMyelin-positive area shows significant increases following remyelination in both WT and YAC128 (two-way ANOVA: interaction $p = 0.8888$, genotype $p = 0.6011$, treatment $p = 0.0049$). **d** Quantification of the intensity of FluoroMyelin staining demonstrates a significant increase following remyelination in WT, but not YAC128, mice (two-way ANOVA: interaction $p < 0.0001$, genotype $p < 0.0001$, treatment $p < 0.0001$). N = 4–7 for WT-DM, 4–8 for WT-RM, 4–7 for YAC128-DM, and 4–7 for YAC128-RM; two-way ANOVA with Fisher's LSD post hoc test. $^{*}p < 0.05$, $^{**}p < 0.01$, $^{***}p < 0.001$, n.s. = not significant. DM = demyelinated, RM = remyelinated

recent study demonstrating altered myelination in response to environmental manipulation (i.e., manipulation of microbiota) in the BACHD mouse model of HD [35].

Deformation and degeneration of myelin sheaths have been shown to develop with aging, even in the absence of specific disease conditions [36, 37]. Neuropathological studies have suggested that axonal damage and degeneration are more likely to occur in demyelinated regions compared with remyelinated ones [38, 39]. The associated loss of WM integrity is increasingly being recognized as a major contributor to age-related cognitive decline [40, 41]. The evidence also links new oligodendrocyte differentiation and de novo myelination in adulthood with the acquisition of new skills such as motor learning [42, 43]. Thus, the ability to renew, replace, and remodel myelin sheaths throughout adulthood is key to healthy brain aging, underscoring the life-long importance of myelin and WM plasticity. In this context, our results of impaired remyelination in YAC128 mice suggest that the neurological manifestations in HD, including the cognitive deficits, may be in part a consequence of compromised WM plasticity in HD.

Many aspects of myelin sheaths and myelination have been shown to be amenable to change in adulthood. These include thickening, thinning, and replacement of existing myelin sheaths, lengthening or shortening of internodal segments as well as de novo myelination of unmyelinated axons and axonal segments [44]. On the cellular level, myelin plasticity and in particular remyelination typically involves activation, migration, and differentiation of oligodendrocyte progenitor cells, the largest population of proliferating cells in the mature CNS, followed by maturation of the newly formed oligodendrocytes [6]. While the different forms of myelin plasticity have been well documented, the mechanisms underlying many of these adaptive and regenerative changes remain to be defined. One mechanism of myelin plasticity that has been shown to influence motor learning is myelin-regulatory factor (MYRF)-dependent oligodendrocyte maturation [42].

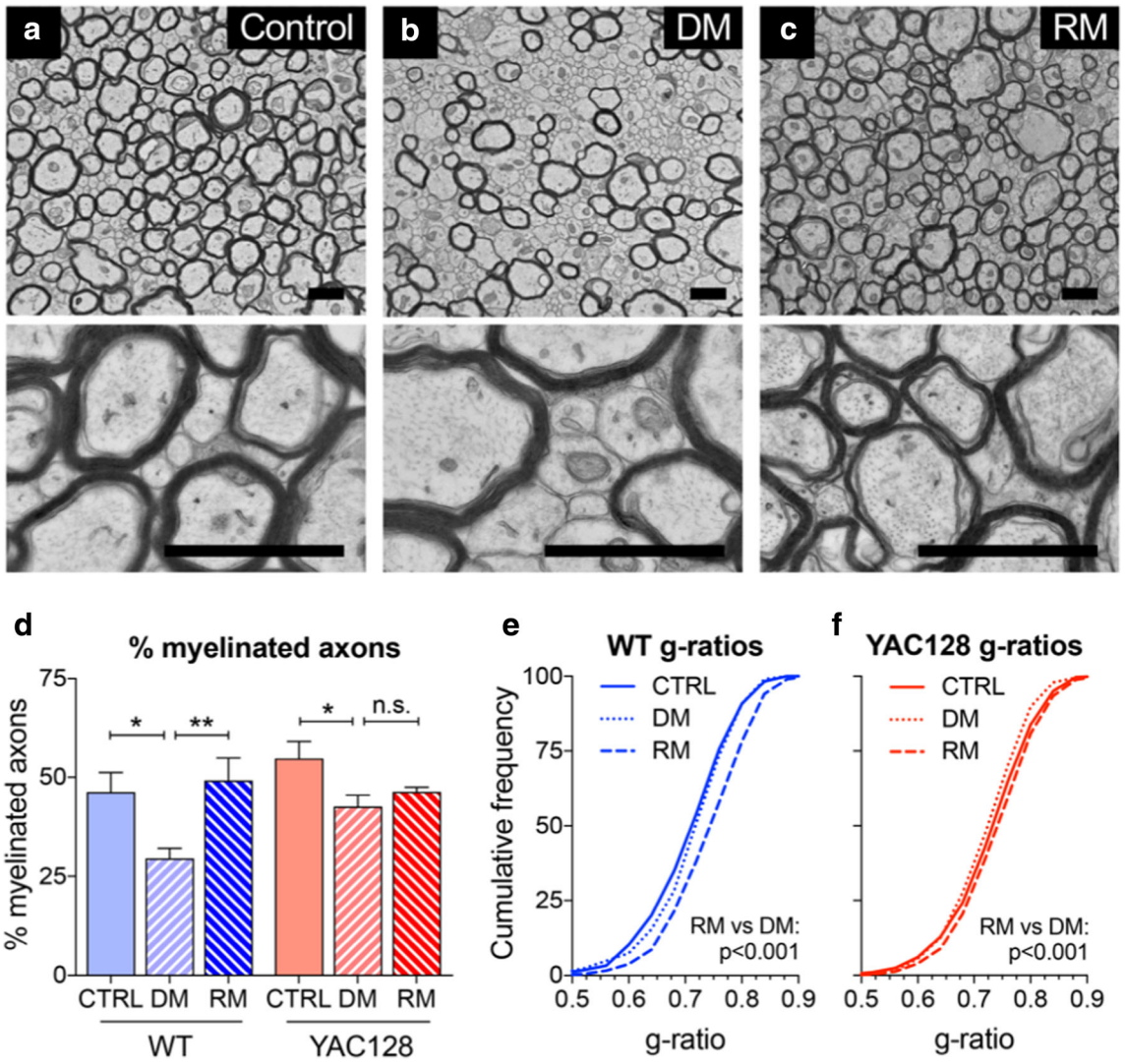

Fig. 4 Ultrastructural analysis of myelinated axons following demyelination and remyelination in the corpus callosum of WT and YAC128 HD mice. **a**–**c** Representative electron microscopy images of the corpus callosum of WT mice belonging to the (**a**) control, (**b**) demyelination, and (**c**) remyelination groups. Scale bar = 1 μm. **d** Cuprizone-induced demyelination resulted in a significant reduction in the percentage of myelinated axons compared to respective controls for both WT and YAC128 HD mice. Following remyelination, the percentage of myelinated axons increased significantly in WT, but not YAC128 HD, mice (one-way ANOVA: $p = 0.0124$). **e**, **f** Cumulative frequency plot of g-ratios following demyelination and remyelination for (**e**) WT and (**f**) YAC128 mice. $N = 3$/group; ~ 150 axons quantified per animal. One-way ANOVA with Fisher's LSD post hoc test for (**d**) and unpaired two-tailed Kolmogorov-Smirnov test for (**e**) and (**f**). $^{*}p < 0.05$, $^{**}p < 0.01$, n.s. = not significant. CTRL = control, DM = demyelinated, RM = remyelinated

Conditional deletion of MYRF in adult mice was shown to blunt the maturation of newly formed oligodendrocytes and impair the ability of the mice to learn a complex motor skill [42, 43]. In animal and cellular models examining oligodendroglial function in HD, the activity of a number of transcription factors involved in oligodendrocyte differentiation and maturation, including MYRF, OLIG2, and SOX10, has been shown to be blunted, an effect that was paralleled by oligodendrocyte dysfunction and hypomyelination [45]. Thus, it is likely that the compromised remyelination response we observe in YAC128 HD mice involves impairments in one or more of these transcriptional regulators of oligodendrocyte differentiation and maturation. Such impairments may also underlie not only the deficits in mature oligodendrocytes counts in YAC128 HD mice we observe at baseline but following remyelination as well.

Myelin membranes comprise the largest pool of free cholesterol in the body [46], and conditions in which cholesterol synthesis is blunted lead to impaired myelination [47]. This signifies the importance of adequate supply of cholesterol for myelin sheath biogenesis and maturation. Deficits in cholesterol metabolism in HD are well-documented [48–51] and have been suggested to be mediated at least in part via impaired PGC1α activity [18, 52, 53], and to contribute to hypomyelination in HD [18, 54]. Our findings of blunted intensity of FluoroMyelin, a lipophilic dye [26], in HD mice at

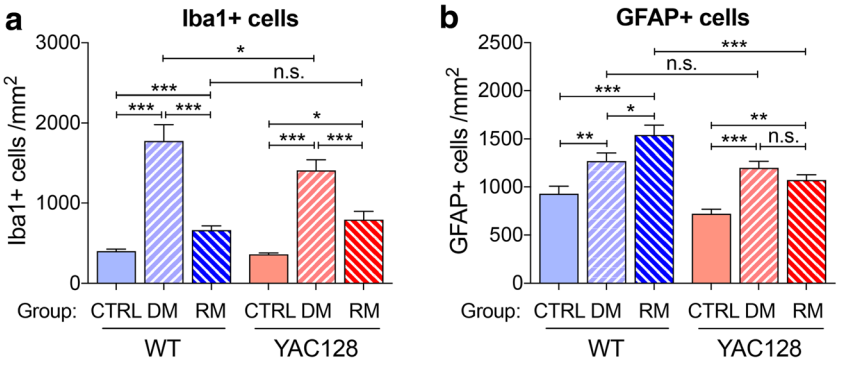

Fig. 5 Glial responses in the corpus callosum following demyelination and remyelination in WT and YAC128 HD mice. **a** Stereological counts of Iba1+ cells show significantly higher infiltration of microglia following demyelination but similar levels following remyelination in WT compared with YAC128 HD mice (one-way ANOVA: $p < 0.0001$). **b** Quantification of GFAP+ cells shows a similar level of astrogliosis following demyelination but a significantly higher level following remyelination in WT compared with YAC128 HD mice (one-way ANOVA: $p < 0.0001$). One-way ANOVA with Fisher's LSD post hoc test. $^{*}p < 0.05$; $^{**}p < 0.01$; $^{***}p < 0.001$, n.s. = not significant. CTRL = control, DM = demyelinated, RM = remyelinated

baseline and following remyelination support the notion of altered myelin lipid composition and suggest that impairment in oligodendroglial function including the capacity to remyelinate is likely to be partly the result of deficits in lipid metabolism. This possibility further suggests that strategies aimed at restoring lipid metabolism [55] may lessen oligodendroglial dysfunction in HD.

In addition to autonomous deficits in oligodendroglia, non-intrinsic factors may also contribute to the impaired remyelination response in YAC128 HD mice. For example, neuronal activity and axonal signals have been shown to promote oligodendrogenesis and to play a key role during myelination, demyelination, and remyelination [56–58]. Similarly, microglia and astrocytes can influence oligodendrocyte differentiation and remyelination efficiency [28, 29, 59, 60]. Mutant HTT has been shown to precipitate a number of synaptic and neuronal aberrations that impact axonal signaling [61]. Moreover, abnormal activity of astrocytes and microglia is also well documented in HD [62, 63]. As such, mutant HTT-mediated abnormalities in axonal signaling, microglial or astrocytic responses may contribute to the impairment in WM plasticity in HD. In our study, the number of callosal astrocytes, but not microglia, was significantly elevated in the remyelinated WT mice compared with the YAC128 HD group, suggesting that differences in the astrocytic response may contribute to the compromised remyelination observed in YAC128 HD mice.

In summary, our study provides evidence that mutant HTT impacts myelination not only during development but also in adulthood, which may impair myelin plasticity and interfere with the repair of age- and disease-related myelin damage in HD. Our findings also raise a number of questions for future studies: to what extent does mutant HTT accelerate the rate of decline in WM plasticity relative to what is observed during normal aging? Which aspects of the disease are most likely to reflect impaired WM plasticity and may therefore benefit from therapeutic approaches targeting this mechanism? In addition to providing insulation and facilitating neurotransmission, oligodendrocytes are a major source of metabolic and trophic support to axons, contributing to their integrity and viability [64, 65]. Hence, do impairments in WM plasticity signify broader deficits in oligodendroglial function such as metabolic and trophic support that may contribute to the axonal degeneration observed in HD? Altogether, our findings support the need for future studies to address the contribution of WM abnormalities to the clinical manifestations of HD and to evaluate their potential as targets for therapy in HD.

Acknowledgements We thank Maria Ericsson (Electron Microscopy Facility, Harvard Medical School) for electron microscopy and the SBIC-Nikon Imaging Centre (A*STAR, Biopolis) for confocal imaging services.

Authors' Contribution R.T.Y.T. and M.A.P. conceived and planned the study. R.T.Y.T., C.F.B., N.A.B.M.Y., C.A.K., and L.J.T. performed experiments. R.T.Y.T. and M.A.P. analyzed data. Y.L.T. provided intellectual input. R.T.Y.T., Y.L.T., and M.A.P. wrote and revised the manuscript.

Funding information C.F.B. is supported by a Singapore International Graduate Award (SINGA) from the Agency for Science, Technology and Research (A*STAR). The work was supported by grants from the Agency for Science, Technology and Research (A*STAR) and the National University of Singapore to M.A.P.

Compliance with Ethical Standards

Conflict of Interest The authors declare that they have no conflict of interest.

References

1. Nave K-A, Werner HB (2014) Myelination of the nervous system: mechanisms and functions. Annu Rev Cell Dev Biol 30:503–533. https://doi.org/10.1146/annurev-cellbio-100913-013101

2. Kessaris N, Pringle N, Richardson WD (2008) Specification of CNS glia from neural stem cells in the embryonic neuroepithelium. Philosophical Transactions of the Royal Society B: Biological Sciences 363:71–85. https://doi.org/10.1098/rstb.2006.2013
3. Rivers LE, Young KM, Rizzi M, Jamen F, Psachoulia K, Wade A, Kessaris N, Richardson WD (2008) PDGFRA/NG2 glia generate myelinating oligodendrocytes and piriform projection neurons in adult mice. Nat Neurosci 11:1392–1401. https://doi.org/10.1038/nn.2220
4. Wang S, Young KM (2014) White matter plasticity in adulthood. Neuroscience 276:148–160. https://doi.org/10.1016/j.neuroscience.2013.10.018
5. Monje M (2018) Myelin plasticity and nervous system function. Annu Rev Neurosci 41:61–76. https://doi.org/10.1146/annurev-neuro-080317-061853
6. Franklin RJM, Ffrench-Constant C (2008) Remyelination in the CNS: from biology to therapy. Nat Rev Neurosci 9:839–855. https://doi.org/10.1038/nrn2480
7. Emery B (2010) Regulation of oligodendrocyte differentiation and myelination. Science 330:779–782. https://doi.org/10.1126/science.1190927
8. Walker FO (2007) Huntington's disease. Lancet 369:218–228. https://doi.org/10.1016/S0140-6736(07)60111-1
9. Vonsattel JP, Myers RH, Stevens TJ et al (1985) Neuropathological classification of Huntington's disease. J Neuropathol Exp Neurol 44:559–577
10. Reiner A, Albin RL, Anderson KD, D'Amato CJ, Penney JB, Young AB (1988) Differential loss of striatal projection neurons in Huntington disease. Proc Natl Acad Sci U S A 85:5733–5737
11. Tabrizi SJ, Langbehn DR, Leavitt BR, Roos RA, Durr A, Craufurd D, Kennard C, Hicks SL et al (2009) Biological and clinical manifestations of Huntington's disease in the longitudinal TRACK-HD study: cross-sectional analysis of baseline data. Lancet Neurol 8:791–801. https://doi.org/10.1016/S1474-4422(09)70170-X
12. Paulsen JS, Nopoulos PC, Aylward E, Ross CA, Johnson H, Magnotta VA, Juhl A, Pierson RK et al (2010) Striatal and white matter predictors of estimated diagnosis for Huntington disease. Brain Res Bull 82:201–207. https://doi.org/10.1016/j.brainresbull.2010.04.003
13. Poudel GR, Stout JC, Domínguez DJF et al (2015) Longitudinal change in white matter microstructure in Huntington's disease: the IMAGE-HD study. Neurobiol Dis 74:406–412. https://doi.org/10.1016/j.nbd.2014.12.009
14. Phillips OR, Joshi SH, Squitieri F, Sanchez-Castaneda C, Narr K, Shattuck DW, Caltagirone C, Sabatini U et al (2016) Major superficial white matter abnormalities in Huntington's disease. Front Neurosci 10:1655–1613. https://doi.org/10.3389/fnins.2016.00197
15. Rosas HD, Wilkens P, Salat DH, Mercaldo ND, Vangel M, Yendiki AY, Hersch SM (2018) Complex spatial and temporally defined myelin and axonal degeneration in Huntington disease. Neuroimage (Amst) 20:236–242. https://doi.org/10.1016/j.nicl.2018.01.029
16. Novak MJU, Seunarine KK, Gibbard CR, Hobbs NZ, Scahill RI, Clark CA, Tabrizi SJ (2014) White matter integrity in premanifest and early Huntington's disease is related to caudate loss and disease progression. Cortex 52:98–112. https://doi.org/10.1016/j.cortex.2013.11.009
17. Carroll JB, Lerch JP, Franciosi S, Spreeuw A, Bissada N, Henkelman RM, Hayden MR (2011) Natural history of disease in the YAC128 mouse reveals a discrete signature of pathology in Huntington disease. Neurobiol Dis 43:257–265. https://doi.org/10.1016/j.nbd.2011.03.018
18. Xiang Z, Valenza M, Cui L, Leoni V, Jeong HK, Brilli E, Zhang J, Peng Q et al (2011) Peroxisome-proliferator-activated receptor gamma coactivator 1 α contributes to dysmyelination in experimental models of Huntington's disease. J Neurosci 31:9544–9553. https://doi.org/10.1523/JNEUROSCI.1291-11.2011
19. Jin J, Peng Q, Hou Z, Jiang M, Wang X, Langseth AJ, Tao M, Barker PB et al (2015) Early white matter abnormalities, progressive brain pathology and motor deficits in a novel knock-in mouse model of Huntington's disease. Hum Mol Genet 24:2508–2527. https://doi.org/10.1093/hmg/ddv016
20. Teo RTY, Hong X, Yu-Taeger L, Huang Y, Tan LJ, Xie Y, To XV, Guo L et al (2016) Structural and molecular myelination deficits occur prior to neuronal loss in the YAC128 and BACHD models of Huntington disease. Hum Mol Genet 25:2621–2632. https://doi.org/10.1093/hmg/ddw122
21. Garcia-Miralles M, Hong X, Tan LJ, Caron NS, Huang Y, To XV, Lin RY, Franciosi S et al (2016) Laquinimod rescues striatal, cortical and white matter pathology and results in modest behavioural improvements in the YAC128 model of Huntington disease. Sci Rep 6:31652. https://doi.org/10.1038/srep31652
22. Garcia-Miralles M, Yusof NABM, Tan JY, Radulescu CI, Sidik H, Tan LJ, Belinson H, Zach N et al (2018) Laquinimod treatment improves myelination deficits at the transcriptional and ultrastructural levels in the YAC128 mouse model of Huntington disease. Mol Neurobiol 130:1759. https://doi.org/10.1007/s12035-018-1393-1
23. Slow EJ, van Raamsdonk J, Rogers D, Coleman SH, Graham RK, Deng Y, Oh R, Bissada N et al (2003) Selective striatal neuronal loss in a YAC128 mouse model of Huntington disease. Hum Mol Genet 12:1555–1567
24. Pouladi MA, Morton AJ, Hayden MR (2013) Choosing an animal model for the study of Huntington's disease. Nat Rev Neurosci 14:708–721. https://doi.org/10.1038/nrn3570
25. Praet J, Guglielmetti C, Berneman Z, van der Linden A, Ponsaerts P (2014) Cellular and molecular neuropathology of the cuprizone mouse model: clinical relevance for multiple sclerosis. Neurosci Biobehav Rev 47C:485–505. https://doi.org/10.1016/j.neubiorev.2014.10.004
26. Monsma PC, Brown A (2012) FluoroMyelin™ red is a bright, photostable and non-toxic fluorescent stain for live imaging of myelin. J Neurosci Methods 209:344–350. https://doi.org/10.1016/j.jneumeth.2012.06.015
27. Duncan ID, Marik RL, Broman AT, Heidari M (2017) Thin myelin sheaths as the hallmark of remyelination persist over time and preserve axon function. PNAS 114:E9685–E9691. https://doi.org/10.1073/pnas.1714183114
28. Lampron A, Larochelle A, Laflamme N, Préfontaine P, Plante MM, Sánchez MG, Yong VW, Stys PK et al (2015) Inefficient clearance of myelin debris by microglia impairs remyelinating processes. J Exp Med 212:481–495. https://doi.org/10.1084/jem.20141656
29. Skripuletz T, Hackstette D, Bauer K, Gudi V, Pul R, Voss E, Berger K, Kipp M et al (2013) Astrocytes regulate myelin clearance through recruitment of microglia during cuprizone-induced demyelination. Brain 136:147–167. https://doi.org/10.1093/brain/aws262
30. Thieben MJ, Duggins AJ, Good CD et al (2002) The distribution of structural neuropathology in pre-clinical Huntington's disease. Brain 125:1815–1828
31. Reading SAJ, Yassa MA, Bakker A, Dziorny AC, Gourley LM, Yallapragada V, Rosenblatt A, Margolis RL et al (2005) Regional white matter change in pre-symptomatic Huntington's disease: a diffusion tensor imaging study. Psychiatry Res 140:55–62. https://doi.org/10.1016/j.pscychresns.2005.05.011

32. Ciarmiello A, Cannella M, Lastoria S, Simonelli M, Frati L, Rubinsztein DC, Squitieri F (2006) Brain white-matter volume loss and glucose hypometabolism precede the clinical symptoms of Huntington's disease. J Nucl Med 47:215–222
33. Rosas HD, Tuch DS, Hevelone ND, Zaleta AK, Vangel M, Hersch SM, Salat DH (2006) Diffusion tensor imaging in presymptomatic and early Huntington's disease: selective white matter pathology and its relationship to clinical measures. Mov Disord 21:1317–1325. https://doi.org/10.1002/mds.20979
34. Stoffers D, Sheldon S, Kuperman JM, Goldstein J, Corey-Bloom J, Aron AR (2010) Contrasting gray and white matter changes in preclinical Huntington disease: an MRI study. Neurology 74:1208–1216. https://doi.org/10.1212/WNL.0b013e3181d8c20a
35. Radulescu CI, Garcia-Miralles M, Sidik H, Bardile CF, Yusof NABM, Lee HU, Ho EXP, Chu CW et al (2019) Manipulation of microbiota reveals altered callosal myelination and white matter plasticity in a model of Huntington disease. Neurobiol Dis 127:65–75. https://doi.org/10.1016/j.nbd.2019.02.011
36. Peters A (2002) The effects of normal aging on myelin and nerve fibers: a review. J Neurocytol 31:581–593
37. Marner L, Nyengaard JR, Tang Y, Pakkenberg B (2003) Marked loss of myelinated nerve fibers in the human brain with age. J Comp Neurol 462:144–152. https://doi.org/10.1002/cne.10714
38. Kornek B, Storch MK, Weissert R, Wallstroem E, Stefferl A, Olsson T, Linington C, Schmidbauer M et al (2000) Multiple sclerosis and chronic autoimmune encephalomyelitis: a comparative quantitative study of axonal injury in active, inactive, and remyelinated lesions. Am J Pathol 157:267–276. https://doi.org/10.1016/S0002-9440(10)64537-3
39. Dutta R, Trapp BD (2011) Mechanisms of neuronal dysfunction and degeneration in multiple sclerosis. Prog Neurobiol 93:1–12. https://doi.org/10.1016/j.pneurobio.2010.09.005
40. Madden DJ, Bennett IJ, Song AW (2009) Cerebral white matter integrity and cognitive aging: contributions from diffusion tensor imaging. Neuropsychol Rev 19:415–435. https://doi.org/10.1007/s11065-009-9113-2
41. Bennett IJ, Madden DJ (2014) Disconnected aging: cerebral white matter integrity and age-related differences in cognition. Neuroscience 276:187–205. https://doi.org/10.1016/j.neuroscience.2013.11.026
42. McKenzie IA, Ohayon D, Li H et al (2014) Motor skill learning requires active central myelination. Science 346:318–322. https://doi.org/10.1126/science.1254960
43. Xiao L, Ohayon D, McKenzie IA et al (2016) Rapid production of new oligodendrocytes is required in the earliest stages of motor-skill learning. Nat Neurosci 19:1210–1217. https://doi.org/10.1038/nn.4351
44. Chang K-J, Redmond SA, Chan JR (2016) Remodeling myelination: implications for mechanisms of neural plasticity. Nat Neurosci 19:190–197. https://doi.org/10.1038/nn.4200
45. Huang B, Wei W, Wang G, Gaertig MA, Feng Y, Wang W, Li XJ, Li S (2015) Mutant huntingtin downregulates myelin regulatory factor-mediated myelin gene expression and affects mature oligodendrocytes. Neuron 85:1212–1226. https://doi.org/10.1016/j.neuron.2015.02.026
46. Saher G, Stumpf SK (2015) Cholesterol in myelin biogenesis and hypomyelinating disorders. Biochim Biophys Acta 1851:1083–1094. https://doi.org/10.1016/j.bbalip.2015.02.010
47. Saher G, Brügger B, Lappe-Siefke C, Möbius W, Tozawa RI, Wehr MC, Wieland F, Ishibashi S et al (2005) High cholesterol level is essential for myelin membrane growth. Nat Neurosci 8:468–475. https://doi.org/10.1038/nn1426
48. Shankaran M, Di Paolo E, Leoni V et al (2017) Early and brain region-specific decrease of de novo cholesterol biosynthesis in Huntington's disease: a cross-validation study in Q175 knock-in mice. Neurobiol Dis 98:66–76. https://doi.org/10.1016/j.nbd.2016.11.013
49. Valenza M, Marullo M, Di Paolo E et al (2015) Disruption of astrocyte-neuron cholesterol cross talk affects neuronal function in Huntington's disease. Cell Death Differ 22:690–702. https://doi.org/10.1038/cdd.2014.162
50. Valenza M, Leoni V, Karasinska JM, Petricca L, Fan J, Carroll J, Pouladi MA, Fossale E et al (2010) Cholesterol defect is marked across multiple rodent models of Huntington's disease and is manifest in astrocytes. J Neurosci 30:10844–10850. https://doi.org/10.1523/JNEUROSCI.0917-10.2010
51. Valenza M, Rigamonti D, Goffredo D, Zuccato C, Fenu S, Jamot L, Strand A, Tarditi A et al (2005) Dysfunction of the cholesterol biosynthetic pathway in Huntington's disease. J Neurosci 25:9932–9939. https://doi.org/10.1523/JNEUROSCI.3355-05.2005
52. Cui L, Jeong H, Borovecki F, Parkhurst CN, Tanese N, Krainc D (2006) Transcriptional repression of PGC-1alpha by mutant huntingtin leads to mitochondrial dysfunction and neurodegeneration. Cell 127:59–69. https://doi.org/10.1016/j.cell.2006.09.015
53. Weydt P, Pineda VV, Torrence AE, Libby RT, Satterfield TF, Lazarowski ER, Gilbert ML, Morton GJ et al (2006) Thermoregulatory and metabolic defects in Huntington's disease transgenic mice implicate PGC-1alpha in Huntington's disease neurodegeneration. Cell Metab 4:349–362. https://doi.org/10.1016/j.cmet.2006.10.004
54. Valenza M, Cattaneo E (2011) Emerging roles for cholesterol in Huntington's disease. Trends Neurosci 34:474–486. https://doi.org/10.1016/j.tins.2011.06.005
55. Valenza M, Chen JY, Di Paolo E et al (2015) Cholesterol-loaded nanoparticles ameliorate synaptic and cognitive function in Huntington's disease mice. EMBO Mol Med 7:1547–1564. https://doi.org/10.15252/emmm.201505413
56. Gibson EM, Purger D, Mount CW, Goldstein AK, Lin GL, Wood LS, Inema I, Miller SE et al (2014) Neuronal activity promotes oligodendrogenesis and adaptive myelination in the mammalian brain. Science. 344:1252304. https://doi.org/10.1126/science.1252304
57. Coman I, Barbin G, Charles P, Zalc B, Lubetzki C (2005) Axonal signals in central nervous system myelination, demyelination and remyelination. J Neurol Sci 233:67–71. https://doi.org/10.1016/j.jns.2005.03.029
58. Piaton G, Gould RM, Lubetzki C (2010) Axon-oligodendrocyte interactions during developmental myelination, demyelination and repair. J Neurochem 114:1243–1260. https://doi.org/10.1111/j.1471-4159.2010.06831.x
59. Miron VE, Boyd A, Zhao J-W, Yuen TJ, Ruckh JM, Shadrach JL, van Wijngaarden P, Wagers AJ et al (2013) M2 microglia and macrophages drive oligodendrocyte differentiation during CNS remyelination. Nat Neurosci 16:1211–1218. https://doi.org/10.1038/nn.3469
60. Claycomb KI, Johnson KM, Winokur PN, Sacino A, Crocker S (2013) Astrocyte regulation of CNS inflammation and remyelination. Brain Sci 3:1109–1127. https://doi.org/10.3390/brainsci3031109
61. Morfini GA, You Y-M, Pollema SL, Kaminska A, Liu K, Yoshioka K, Björkblom B, Coffey ET et al (2009) Pathogenic huntingtin inhibits fast axonal transport by activating JNK3 and phosphorylating kinesin. Nat Neurosci 12:864–871. https://doi.org/10.1038/nn.2346

62. Khakh BS, Beaumont V, Cachope R, Munoz-Sanjuan I, Goldman SA, Grantyn R (2017) Unravelling and exploiting astrocyte dysfunction in Huntington's disease. Trends Neurosci 40:422–437. https://doi.org/10.1016/j.tins.2017.05.002
63. Andre R, Carty L, Tabrizi SJ (2015) Disruption of immune cell function by mutant huntingtin in Huntington's disease pathogenesis. Curr Opin Pharmacol 26:33–38. https://doi.org/10.1016/j.coph.2015.09.008
64. Fünfschilling U, Supplie LM, Mahad D, Boretius S, Saab AS, Edgar J, Brinkmann BG, Kassmann CM et al (2012) Glycolytic oligodendrocytes maintain myelin and long-term axonal integrity. Nature 485:517–521. https://doi.org/10.1038/nature11007
65. Lee Y, Morrison BM, Li Y, Lengacher S, Farah MH, Hoffman PN, Liu Y, Tsingalia A et al (2012) Oligodendroglia metabolically support axons and contribute to neurodegeneration. Nature 487:443–448. https://doi.org/10.1038/nature11314